

or purified antibodies was added to the plates for 1-h incubation at 37°C. Plates were rewashed with PBST, 100 µl of alkaline phosphatase (AP)-conjugated goat anti-mouse Fab specific antibody (1:1000 dilution, Sigma-Aldrich) was added, and the plates were incubated for an additional 1 h at 37°C. Unbound AP conjugate was washed away with PBST, bound antibodies were detected by incubation for 1 h at 37°C with a *p*-nitrophenyl phosphate (pNPP) substrate (Bio-Rad), and OD<sub>405-620</sub> was read. ELISA antibody titer was expressed as the highest dilution giving an OD<sub>405-620</sub> of 0.1 unit higher than that of the control wells without antigen.

ELISA plates were coated with an anti-mouse Fab antibody (0.5 µg/well; Sigma-Aldrich). Then the test samples were added to the plates incubated for 1 h at 37°C, followed by blocking with 3% skim milk in PBS. Serially diluted mouse Fab (Jackson ImmunoResearch Laboratories, West Grove, PA, USA) was used as a standard in all assays. After incubation, AP-conjugated anti-mouse Fab antibody (1:1000 dilution, Sigma-Aldrich) was added and the plates were incubated for an additional 1 h at 37°C. The plates were washed and incubated with a pNPP substrate (Bio-Rad) for 1 h at 37°C and the OD<sub>405-620</sub> was read.

**Purification of Fab fragments** The filtered protein solutions were loaded onto a Ni<sup>2+</sup>-charged-5 ml HiTrap Chelating HP column (GE Healthcare Bio-Sciences, Piscataway, NJ, USA) at a flow rate of 5 ml/min using a chromatography system (BIO CAD sprint; Applied Biosystems Japan). After washing with 20 column volumes of PBS/5 mM imidazole, the bound protein was eluted with 5 column volumes of PBS/500 mM imidazole. The eluate was concentrated and the buffer was exchanged to PBS using a 30-kDa-molecular-size cut-off filter (CentriPlus; Millipore, Billerica, MA, USA), and filtered through 0.22-µm filters.

**Kinetics studies** Biacore 3000 (Biacore AB, Uppsala, Sweden) based on the principle of surface plasmon resonance was used to compare antibodies. The lysine-linked tandem repeat peptide antigen of KH5, TYEAALKQYEADLKKT YEAAALKQYEADL (3), was immobilized on the sensor chip CM5. Bovine serum albumin (BSA; Sigma-Aldrich) was also immobilized as a negative control. Antibody samples were suspended in HBS-EP buffer (Biacore AB). Each sample was injected onto the sensor at 3.12, 6.25, 12.5, 25 and 50 nM at 30 µl/min for 120 s, followed by an injection of HBS-EP buffer. The kinetics was determined using BIAevaluation 3.2 (Biacore AB).

## RESULTS

### Cloning of Fab genes and generation of transgenic cells

The cDNAs coding for the Fab H and L chains were cloned into the pFab-His2 vector (9). To identify bacterial clones expressing the Fab fragments of interest, their reactivity to Pac was tested by ELISA. The most reactive of the positive clones, T15, was used for subsequent studies. The data in Fig. 1 show that expression was controlled by the *E. coli* *tac* promoter and the Shine-Dalgarno sequence (*tac*-SD). The *pelB* signal peptides (*pelB*) directed the Fab fragments into the periplasmic space of the bacterial host (9). The 6x histidine tag sequence was fused to the C-terminal of the Fab H chain.

The cDNAs of the Fab H and L chains were transferred from pT15, the plasmid containing cDNA of the T15 Fab fragment, to the pBI 101 binary vector for the transformation of tobacco cells (Fig. 1). The ER retention signal sequence, KDEL, which is reported to enhance the production of recombinant proteins (12), was added at the C-terminal region of Fab in the p24 and p26 constructs to investigate its

effects on increasing antibody recovery. The secretion signal of *Nicotiana plumbaginifolia* was also used to direct Fab fragments to the secretion pathway in the p25 and p26 constructs (10). Four series of transgenic tobacco XD6S suspension cells (X23, X24, X25 and X26) were obtained by *Agrobacterium*-mediated transformation with the corresponding binary plasmids.

### Characterization of transgenic tobacco cell lines

Between 10 and 20 kanamycin-resistant clones of each transgenic line were grown in a small liquid media and the total protein extracts from 1-ml cultures (including the proteins in the cells and media) were tested by anti-Pac ELISA. The data in Fig. 2 show the OD of each transgenic clone. The X23 and X24 clones had no anti-Pac activity. Many X25 clones showed higher ODs, which meant that they produced more anti-Pac Fabs per ml of culture, than the X26 clones. The X25-3 and X26-2 cell lines, with specific cell lines designated after the hyphen, were selected for further analysis because their ELISA ODs were higher than those of the other cell lines. Both cell lines grew as well as their parental XD6S cells.

The time courses of the anti-Pac activities and amounts of mouse Fab fragments were quantified from the TSP concentrations (Fig. 3). The Fab fragments were quantified by sandwich ELISA with anti-mouse Fab fragment antibodies. The anti-Pac titers, mouse Fab fragments and TSPs all showed similar time courses of production, with peak titers observed 10 to 14 d after inoculation. The X25-3 cell line had higher TSP concentrations, anti-Pac titers, and Fab amounts than the X26-2 cell line.

**Recovery of Fab fragments from cultures** The X25-3 and X26-2 cell lines were cultured for the recovery of the Fab fragments, designated X253 and X262. About 2 mg/l Fab fragments were detected from both cell extracts, but their amount in the culture media differed between X25-3 and X26-2 (Fig. 4A). The X253 Fab fragment was secreted into the media at levels greater than 10 mg/l, but X263 was secreted at levels less than 1 mg/l. The tobacco cell culture medium had only 0.1–0.4 g/l TSP in the 10-d culture of X25-3 and the ratio of the X253 Fab fragment to TSP was

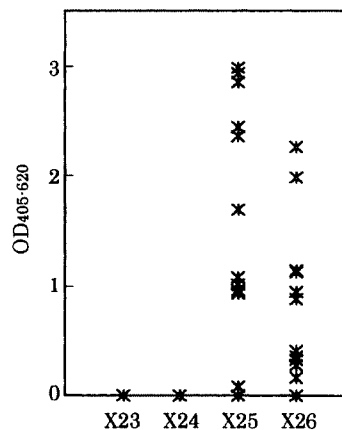


FIG. 2. Anti-Pac ELISA of transgenic tobacco clones. Between 10 and 20 clones of each transgenic cell lines X23, X24, X25 and X26, were inoculated for 7 d. Protein extracts were prepared from 1 ml of culture of each clone and the anti-Pac activity of each clone was measured by ELISA. OD<sub>405-620</sub> values were plotted.

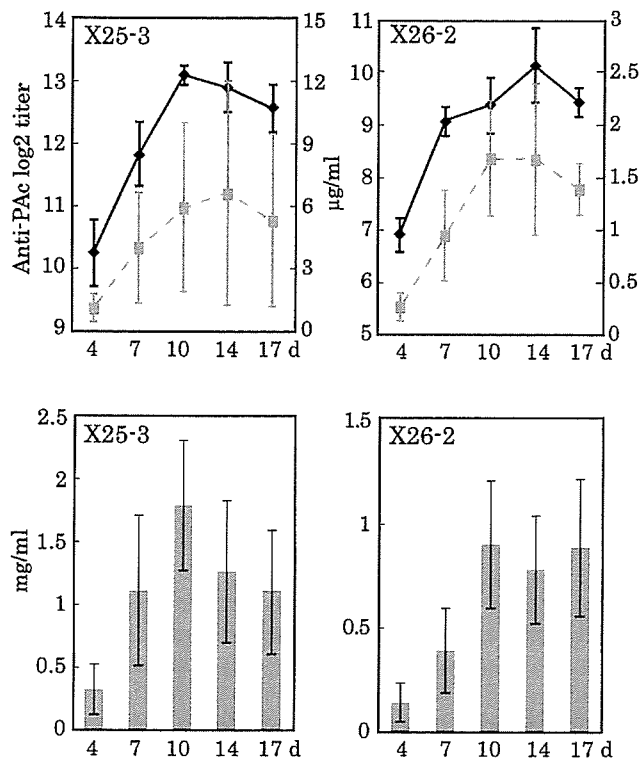


FIG. 3. Time course of antibody production in transgenic cell lines. X25-3 and X26-2 cultures were sampled from 4 to 17 d after inoculation. Both anti-PAC titer (black lines) and the amount of mouse Fab fragment (gray dashed lines) in samples were measured by ELISA. Total soluble protein concentration (gray bars) was measured by the Bradford assay. The results are presented as mean  $\pm$  s.d. ( $n=3$ ).

about 1:10 (w/w). In both the X25-3 and X26-2 cell extracts and in the media of X26-2, the amounts of Fab fragments were only 0.1–0.5% of the TSP concentrations.

Ten-day cultures of 100 ml of tobacco suspension cells were processed, and Fab fragments were recovered on a  $\text{Ni}^{2+}$  ion column via their affinity to the  $6 \times$  His tag. Fab fragments from X26-2 cultures or X25-3 cell extracts were difficult to recover in sufficient amounts for further analysis. However, we did recover the X253 Fab fragment from the culture medium of X25-3. The T15 Fab fragment was also recovered from a  $\text{Ni}^{2+}$  column and the original mouse KH5 MAb was recovered from a protein A column using standard methods (10). Five micrograms of protein from the T15 and X253  $\text{Ni}^{2+}$  column effluents, the KH5 effluents of the protein A column and 5  $\mu\text{g}$  of protein from the  $\text{Ni}^{2+}$  column effluent from the X26-2 media as a negative control were subjected to 12.5% SDS-PAGE for analysis (Fig. 4B) (13). The heavy- and light-chain bands, indicated by open arrowheads, were mainly in the KH5 sample. Many extra bands were detected in the T15 and X253 samples. Proteins over 100 kDa in size in the media, particularly for X253 and X262, bound to the  $\text{Ni}^{2+}$  ion or resin of the column. The quantity of the Fab fragments increased from about 10% of TSP in the culture medium to about 30% of TSP in the column effluent. The molecular sizes, as deduced from the amino acid sequence, were calculated to be 25 kDa for the heavy chain and 24 kDa for the light chain of both T15 and

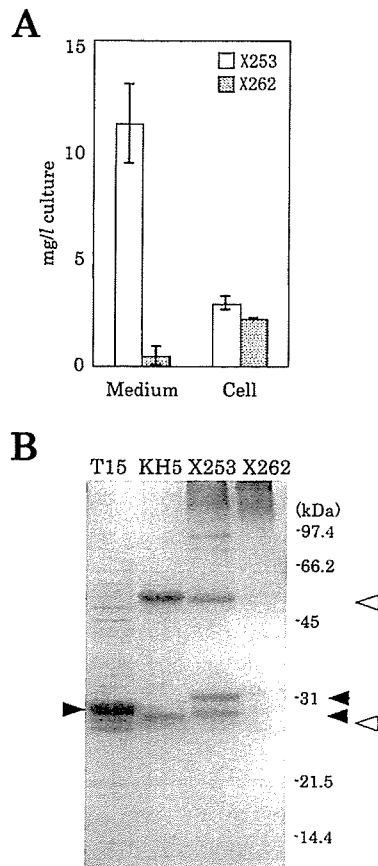


FIG. 4. Recovery of Fab fragments from transgenic cell lines. (A) X253 and X262 Fab fragments in either media or cell extracts. The media and cell extracts of 10-d cultures were prepared. The X253 and X262 mouse Fab fragments were quantified by ELISA. The results are presented as mean  $\pm$  s.d. ( $n=3$ ). (B) SDS-PAGE analysis of antibodies. Purified KH5 (from hybridoma: open triangles), T15 (from *E. coli* extracts: closed triangles at the left side of the gel), X253 (from culture media: closed triangles at the right side of the gel) and the  $\text{Ni}^{2+}$  column effluent of X26-2 media were analyzed using 12.5% SDS-PAGE.

X253. However, the putative bands were larger on the gel; specifically, 28 kDa doublet bands of T15 and 27 and 31 kDa bands of X253 were detected. It has been reported that Fab H and L chains expressed by a pFab1-His2 vector tend to be somewhat larger than expected on the basis of the deduced sequence (9). An approximately 50-kDa band of X253 might have been the H and L chain assembled into the Fab form. Two other bands were also observed at about 80 to 90 kDa that seemed to be three times the size of the X253 Fab H and/or L bands.

**Kinetic studies** Antigen binding activity was compared among the antibodies by ELISA (Fig. 5). KH5, T15 and X253 were the same samples used for SDS-PAGE shown in Fig. 4. The X25-3 medium was from a 10-d post inoculation culture. Antibodies were quantified by sandwich ELISA and then serially diluted over the same range used for the quantitative comparison of the ELISA PAC binding activities. The molecular mass of KH5 is 3 times larger than that of T15 or the X253 Fab and there are two antigen binding sites on KH5 compared with one on the Fab fragments. All antibodies showed similar curves on the graph, despite the

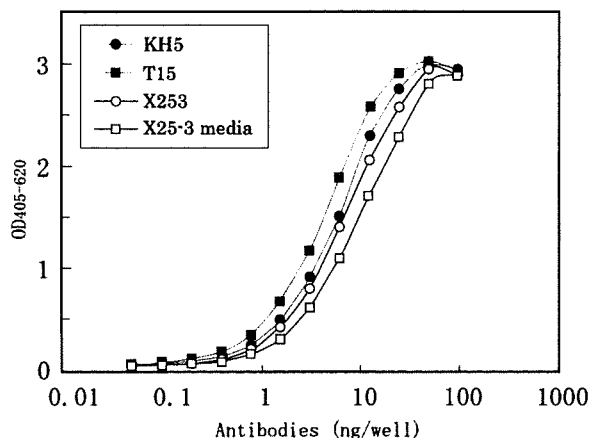


FIG. 5. Quantitative analysis of purified antibodies. Serially diluted solutions of KH5 (closed circles), T15 (closed squares), X253 (open circles) and media of X25-3 (open squares) cells were analyzed using anti-PAc ELISA. The means of triplicate experiments are shown.

difficulties in making a direct comparison of binding activities.

To precisely compare the antibodies, Biacore 3000 was used to determine dissociation constant (KD: Table 1). The di-lysine-linked tandem repeat peptide of the antigen was immobilized on a sensor chip to investigate the interaction with antibodies. Concentration-dependent antibody-antigen interactions, which supported the specificities of the antibodies, were detected and no interactions were detected between BSA and antibodies (data not shown). The association rates ( $k_a$ ) of antibodies were approximately the same, but the dissociation rate ( $k_d$ ) varied from  $2.2 \times 10^{-5}$  to  $1.3 \times 10^{-3} \text{ s}^{-1}$ . The variation in  $k_d$  had an effect on the differences of KDs, which is defined as  $k_d/k_a$ . KD values indicated that the strengths of the affinities were in the order  $\text{KH5} > \text{T15} > \text{X253} > \text{media}$ , with KH5 having the highest affinity. Considering the differences between IgG and Fab, the KD values are appropriate.

## DISCUSSION

Many recombinant antibodies are being developed for use as therapeutic antibodies (14). Antibodies function as a component of the immune system. Specific targets, such as cancer tissues or viruses, are destroyed via complement-dependent cytotoxicity (CDC), antibody-dependent cellular cytotoxicity (ADCC) or neutralization (15). Small antibodies, Fab or scFv, are applicable as targeting tools for the DDS (5). To clone the cDNA of antibodies, *E. coli* is a useful host, but it cannot produce large proteins or antibacterial peptides. Plant cells are potentially good hosts for the production of antibodies if the antibodies are fused with antibacterial peptides (7, 10, 16, 17). The *E. coli* system described in this study has been well established and we have published our experiences with cloning and producing several antibodies using this system (9, 18, 19). Usually, 10 mg of soluble Fab fragments was recovered from 1 l of *E. coli* cultures. In this study, we obtained approximately the same amount of soluble Fab fragments in the culture media as shown in Fig. 4. This result indicates that plant culture sys-

TABLE 1. Kinetic interactions between antibodies and PAc peptide

Sample tested	$k_a$ ( $\text{M}^{-1} \text{ s}^{-1}$ )	$k_d$ ( $\text{s}^{-1}$ )	KD (M)
KH5	$2.4 \times 10^5$	$2.2 \times 10^{-5}$	$9.1 \times 10^{-11}$
T15	$4.0 \times 10^5$	$5.0 \times 10^{-4}$	$1.3 \times 10^{-9}$
X253	$3.2 \times 10^5$	$9.1 \times 10^{-4}$	$2.9 \times 10^{-9}$
X25-3 media	$3.6 \times 10^5$	$1.3 \times 10^{-3}$	$3.7 \times 10^{-9}$

tems are candidates for the production of small antibodies and their derivatives.

The addition of the ER retention signal, the KDEL tetrapeptide, to the C-terminal of the protein is a standard method for the enhancement of protein production in plant cells (12). When KDEL was fused at the C terminus, the expression levels of scFv were one to two orders of magnitude higher than those of scFv without KDEL (12). The Fab X262 has a KDEL motif at the C terminus of both the H and L fragments. However, these signals did not enhance the accumulation of X262 in the cells, but prevented the secretion of X262 into the culture media because of ER retention. However, X253 was actively secreted into the media. The plant cell culture media mainly contained sucrose, minerals and plant hormones and Fab fragments constitute about 10% of the TSP levels. Defects in Fab production in the X23 and X24 series pointed to the importance of protein secretion signals. The Fab fragment has a disulfide bond between the H and L chains, which is formed in the secretion pathway (20). When we use XD6S cells for antibody production, protein recovery from the media might be more efficient than recovering proteins that have accumulated in the ER.

$\text{Ni}^{2+}$  columns did not work well for trapping the Fab fragments containing a 6x His tag at the C-terminal of H chains. Particularly for plant cell cultures, many proteins and carbohydrates may bind to the  $\text{Ni}^{2+}$  column, including some substances that bind non specifically to the carrier of the ion. We were unable to improve either the purity or recovery rate of Fab fragments, despite the use of stringent wash conditions for the  $\text{Ni}^{2+}$  column. Other affinity purification procedures, possibly antigen or anti-Fab antibody columns, should be tried to achieve efficient recovery. In the culture media, there are some impurities that affect the dissociation of Fab from the antigen, because  $k_d$  differs between the media and X253. However these impurities do not influence the association of the Fab with the antigen, because the  $k_a$  of the media is almost the same as that of X253. This finding means that we can use media containing an antibody as antibody reagents without purification if the end use of the Fabs is in *in vitro* examination.

The binding specificities and affinities were similar among antibodies from mouse hybridomas, *E. coli* and cultured tobacco cells. However, the size of each antibody fragment was different from that deduced from the amino acid sequences. Some modifications, e.g., *N*-glycosylation, should be considered; however, there are no experimental data to explain the differences between the band sizes of T15 and X253.

In conclusion, some aspects of the production of Fab fragments by plant cell culture need further improvement, such as the recovery of Fab fragments. However, plant sys-

tems have unique properties that allow the secretion of Fabs to their media, with only a limited secretion of proteins from cells. If we can utilize these characteristics effectively, plant cells will become a powerful tool for the production of small antibodies.

### ACKNOWLEDGMENTS

This work was supported by grants from the Ministry of Health, Labor and Welfare of Japan.

### REFERENCES

1. **Takahashi, I., Okahashi, N., Matsushita, K., Tokuda, M., Kanamoto, T., Munekata, E., Russell, M., and Koga, T.:** Immunogenicity and protective effect against oral colonization by *Streptococcus mutans* of synthetic peptides of a streptococcal surface protein antigen. *J. Immunol.*, **146**, 332–336 (1991).
2. **Ma, J. K. C., Hikmat, B. Y., Wycoff, K., Vine, N. D., Chargelegue, D., Yu, L., Hein, M. B., and Lehner, T.:** Characterization of a recombinant plant monoclonal secretory antibody and preventive immunotherapy in humans. *Nat. Biotechnol.*, **4**, 601–606 (1998).
3. **Yano, A., Onozuka, A., Matin, K., Imai, S., Hanada, N., and Nisizawa, T.:** RGD motif enhances immunogenicity and adjuvanticity of peptide antigens following intranasal immunization. *Vaccine*, **22**, 237–243 (2003).
4. **Senpuku, H., Kato, H., Takeuchi, H., Noda, A., and Nisizawa, T.:** Identification of core B cell epitope in the synthetic peptide inducing cross-inhibitory antibodies to a surface protein antigen of *Streptococcus mutans*. *Immunol. Invest.*, **26**, 531–548 (1997).
5. **Park, J. W.:** Liposome-based drug delivery in breast cancer treatment. *Breast Cancer Res.*, **4**, 95–99 (2002).
6. **Hamilton, I. R.:** Ecological basis for dental caries, p. 219–274. In Kuramitsu, H. K. and Ellen, R. P. (ed.), *Oral bacterial ecology: the molecular basis*. Horizon Scientific Press, Norfolk (2000).
7. **Peschen, D., Li, H. P., Fischer, R., Kreuzaler, F., and Liao, Y. C.:** Fusion proteins comprising a *Fusarium*-specific antibody linked to antifungal peptides protect plants against a fungal pathogen. *Nat. Biotechnol.*, **22**, 732–738 (2004).
8. **Nölke, G., Fischer, R., and Schillberg, S.:** Production of therapeutic antibodies in plants. *Expert Opin. Biol. Ther.*, **3**, 1153–1162 (2003).
9. **Maeda, T., Nagatsuka, Y., Ihara, S., Aotsuka, S., Ono, Y., Inoko, H., and Takekoshi, M.:** Bacterial expression of a human recombinant monoclonal antibody Fab fragment against hepatitis B surface antigen. *J. Med. Virol.*, **58**, 338–345 (1999).
10. **Yano, A., Maeda, F., and Takekoshi, M.:** Transgenic tobacco cells producing the human monoclonal antibody to hepatitis B virus surface antigen. *J. Med. Virol.*, **73**, 208–215 (2004).
11. **Yamaoka, T., Hayashi, T., and Sato, S.:** Secretion of enzymes by plant cells cultured *in vitro*. *J. Fac. Sci. Univ. Tokyo Sect.*, **2**, 117–127 (1969).
12. **Conrad, U. and Fiedler, U.:** Compartment-specific accumulation of recombinant immunoglobulins in plant cells: an essential tool for antibody production and immunomodulation of physiological functions and pathogen activity. *Plant Mol. Biol.*, **38**, 101–109 (1998).
13. **Laemmli, U. K.:** Cleavage of structural proteins during the assembly of the head of bacteriophage T4. *Nature*, **227**, 680–685 (1970).
14. **Breedveld, F. C.:** Therapeutic monoclonal antibodies. *Lancet*, **355**, 735–740 (2000).
15. **Fonsatti, E., Giacomo, A. M. D., and Maio, M.:** Optimizing complement-activating antibody-based cancer immunotherapy: a feasible strategy? *J. Transl. Med.*, **2**, 21–23 (2004).
16. **Ma, J. K. C., Drake, P. M. W., and Christou, P.:** The production of recombinant pharmaceutical proteins in plants. *Nat. Rev. Genet.*, **4**, 794–805 (2003).
17. **Yano, A. and Takekoshi, M.:** Transgenic plant-derived pharmaceuticals — the practical approach? *Expert Opin. Biol. Ther.*, **4**, 1565–1568 (2004).
18. **Takekoshi, M., Maeda, F., Tachibana, H., Inoko, H., Kato, S., Takakura, I., Kenjyo, T., Hiraga, S., Ogawa, Y., Horiki, T., and Ihara, S.:** Human monoclonal anti-HCMV neutralizing antibody from phage display libraries. *J. Virol. Methods*, **74**, 89–98 (1998).
19. **Maeda, F., Takekoshi, M., Nagatsuka, Y., Aotsuka, S., Tsukahara, M., Ohshima, A., Kido, I., Ono, Y., and Ihara, S.:** Production and characterization of recombinant human anti-HBs Fab antibodies. *J. Virol. Methods*, **127**, 141–147 (2005).
20. **Frigerio, L., Vine, N. D., Pedrazzini, E., Hein, M. B., Wang, F., Ma, J. K. C., and Vitale, A.:** Assembly, secretion, and vacuolar delivery of a hybrid immunoglobulin in plants. *Plant Physiol.*, **123**, 1483–1493 (2000).

○馬場陽子<sup>1)</sup>、山田奈保子<sup>1)</sup>、大森孝一<sup>2)</sup>

- 1) 福島県総合療育センター 耳鼻咽喉科、  
2) 福島県立医科大学 医学部 耳鼻咽喉科

### 【はじめに】

福島県では平成13年頃から産科医療機関において私的に新生児聴覚スクリーニングが行われるようになり、また平成16年1月からは一部の地域で公的なスクリーニングも開始され、当科にも精査のためrefer児が紹介されるようになった。最近3年間に、新生児聴覚スクリーニング後の精査目的で紹介された症例16名につき受診後の経過について報告する。

### 【対象】

平成15年4月～平成18年3月までに新生児聴覚検査でreferとなり当科に紹介された乳幼児16名。現在の年齢は6ヶ月から4歳1ヶ月、性別は男児10名、女児6名である。

### 【当科での検査、療育の流れ】

1. 初診時は顕微鏡下での鼓膜、外耳道所見の観察、BOA、CORまたは遊戯聴力検査（受診時期に応じた聴力検査）、津守式発達検査。原則として難聴の診断が確定するまでは1ヶ月1回程度、受診し、聴力検査を行う。生後6ヶ月まではAABRの再検査も併用した。AABR両側passした場合はその時点で経過観察は終了とした。
2. 生後3ヶ月以降にASSR、ABRを行い、聴力検査の結果と矛盾がなく、家族の同意もえられれば補聴器をフッティングし、経過観察する。保護者の訴え、聴力検査と脳波による検査に矛盾がある場合には引き続き検査のみで経過観察を行う。難聴が確定した時点で療育に移行する。

### 【検討項目】

1. 初診時期、スクリーニング機器、refer耳
2. 難聴確定時の年齢、初診時の聴力との比較
3. 診断確定後の経過

### 【結果】

#### 1. 初診時期

1ヶ月…4人、2ヶ月…2人、3～6ヶ月…4人、6～12ヶ月…5人、1歳以降…1人他の耳鼻咽喉科を受診しないで産婦人科から直接を紹介されたものは3人で、1ヶ月で受診していた。他の13人は当科以外の耳鼻咽喉科でABRやASSRを受けてから紹介されていた。

スクリーニング機器      AABR…7人、OAE…9人

Refer耳      両側…11人、片側…5人

#### 2. 診断確定年齢

2ヶ月…1人、3ヶ月…1人、6ヶ月…2人、7ヶ月…1人、10ヶ月…1人、1歳0ヶ月…4人、1歳2ヶ月…1人、1歳4ヶ月…1人、1歳7ヶ月…1人、経過観察中…1人

初診から診断確定まで平均6ヶ月を要していた。

#### 初診時の聴力と確定後の聴力

5症例において初診時の聴力評価と経過観察後の聴力評価に差が見られた。3症例は難聴

診断確定後の聴力より閾値が低く、2症例は閾値が高く出たが、5例とも経過観察後の聴力評価はASSRの結果に近いものになった。

### 3. 経過

症例5は2ヶ月でAABR両側 pass したため、その時点で聴覚障害なしと診断した。1歳4ヶ月で診断確定した高度難聴児（症例2）は2歳4ヶ月で人工内耳埋め込みを行った。高度難聴と確定診断された2例（症例9、11）は人工内耳装用に向けて訓練中である。両側難聴が確定した症例は症例15を除き、補聴器を装用し訓練中であるが、症例15については中等度難聴であり、補聴器なしでもある程度音に対する反応があることから保護者の同意が得られないため引き続き経過観察中である。

#### 【考察】

福島県では新生児聴覚スクリーニングを行っている産科医療機関に対し、出生後入院中にreferの場合は1ヶ月健康診査時に再検査することを推奨していることから生後1ヶ月以内に受診した症例はいなかった。産科医療機関からABRのある他の耳鼻咽喉科へ紹介された場合はABRを施行された後に当科へ紹介されたために初診が3ヶ月以降である症例が16例中10例と多かった。診断確定までには初診から平均して6ヶ月を要しており、初診時のBOAやCORのよる評価が難しいことがわかる。初診時のBOAまたはCORの結果とASSR、ABRの結果が不一致な場合、CORや遊戯聴力検査の結果が徐々にASSRの結果に近づく傾向があったことから他覚的な聴力検査であるASSRは乳幼児の難聴の評価に有用であった。自験例では高度難聴児は3例（症例2、9、11）であった。症例2は初診年齢が1歳1ヶ月であったため早期診断とはいえないが、症例9、11については3ヶ月、7ヶ月で診断確定できた。また、中等度難聴児、片側難聴児は1歳7ヶ月までに診断されており明らかにスクリーニングが導入される以前より早期に診断が確定し、療育に移行していると思われた。

表1. 症例のまとめ(聴力は4分法:dB)

症例	性	スクリーニング	refer 耳	初診年齢	診断確定年齢	初診聴力評価	現在聴力評価	ASSR(推定聴力)	診断
1	男	AABR	両	9m	1y7m	COR40	右50左50	右55左60	両感難
2	男	OAE	右	1y1m	1y4m	COR40	右100左90	右100左97.5	両感難
3	女	OAE	両	1m	1y0m	BOA反応良	右50左50	右45左50	両感難
4	女	OAE	両	8m	10m	COR40	ビーブショウ45	右110以上左40	両感難
5	男	AABR	両	1m	2m	BOA反応良	未検査	未検査	異常なし
6	男	OAE	左	11m	1y6m	COR20	COR30	右45左110	左感難
7	女	AABR	左	1m	1y2m	COR80	COR25	未検査	左感難
8	女	OAE	両	6m	1y0m	COR80	ビーブショウ60	右55左47.5	両感難
9	女	AABR	両	1m	3m	BOA反応不良	COR100	右95左100	両感難
10	男	OAE	右	11m	1y0m	COR25	COR25	右95左145、410	右感難
11	男	AABR	両	3m	7m	COR60	COR100	右105左110以上	両感難
12	男	AABR	両	10m	1y0m	COR70	COR45	右20左25	両途中
13	男	AABR	両	4m	7m	COR65	COR70	右75左80	両感難
14	男	OAE	両	2m	経過観察中	COR45	COR45	右15左30	両難聴疑
15	女	OAE	両	2m	6m	BOA反応不良	COR60	右50左80	両感難
16	男	OAE	左	5m	6m	COR40	COR40	右75左55	左感難

厚生労働科学研究・研究成果等啓発事業による成果発表会  
**一般公開講座「難聴とウイルス」**  
ウイルスできこえが悪くなる！なぜ、どうして？

日時：平成19年3月11日(日) 13:00～16:00

場所：エスパル福島 5階ネクストホール（JR福島駅東口）

主催 公立大学法人 福島県立医科大学医学部耳鼻咽喉科  
共催 財団法人 長寿科学振興財団  
日本耳鼻咽喉科学会福島県地方部会

厚生労働科学研究・研究成果等普及啓発事業による成果発表会

一般公開講座

入場無料

# 難聴とウイルス

ウイルスで聞こえが悪くなる！なぜ、どうして？

日時

平成19年

**3/11**日

13:00～15:00

▶ 講演

15:00～16:00

▶ 医療相談

会場

**エスパル福島**  
5階ネクストホール  
(福島駅東口)

主催

公立大学法人福島県立医科大学医学部耳鼻咽喉科

共催

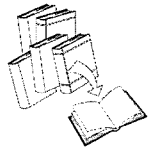
財団法人長寿科学振興財団  
日本耳鼻咽喉科学会福島県地方部会

※医療相談：テーマである「難聴」に関する質問にお答えします。氏名・職業・電話・FAX番号・質問を明記の上、FAXでお申込み下さい。  
締切：平成19年2月末日 FAX番号 024-548-3011

※十分にお席をご用意しておりますが、席に限りがございますので、満席の場合には入場をお断りする場合がございますので、予めご了承下さい。



## REVIEW



## Neuropathogenesis in cytomegalovirus infection: Indication of the mechanisms using mouse models

Yoshihiro Tsutsui\*, Isao Kosugi and Hideya Kawasaki

Department of Pathology, Hamamatsu University School of Medicine, Hamamatsu 431-3192, Japan

### SUMMARY

Cytomegalovirus (CMV) is the most frequent infectious cause of developmental brain disorders and also causes brain damage in immunocompromised individuals. Although the brain is one of the main targets of CMV infection, little is known about the neuropathogenesis of the brain disorders caused by CMV in humans because of the limitations in studying human subjects. Murine CMV (MCMV) is similar to human CMV (HCMV) in terms of genome structure, pattern of gene expressions, cell tropism and infectious dynamics. In mouse models, it has been shown that neural stem/progenitor cells are the most susceptible to CMV infection in developing brains. During brain development, lytic infection tends to occur in immature glial cells, presumably causing structural disorders of the brain. In the prolonged phase of infection, CMV preferentially infects neuronal cells. Infection of neurons may tend to become persistent by evasion of immune reactions, anti-apoptotic effects and neuron-specific activation of the e1-promoter, presumably causing functional neuronal disorders. It has also been shown that CMV infection in developing brains may become latent in neural immature cells. Brain disorders may occur long after infection by reactivation of the latent infection. Copyright © 2005 John Wiley & Sons, Ltd.

Received: 25 March 2005; Revised: 9 May 2005; Accepted: 11 May 2005

### INTRODUCTION

Cytomegalovirus (CMV), a member of the herpes virus group, is the most significant infectious cause of congenital anomalies in the central nervous system (CNS) caused by intrauterine infection in humans, with an average incidence of approximately 1.0% live births [1–4]. It is estimated that approximately 5%–10% of infected infants have generalised cytomegalic inclusion disease at birth, with symptoms such as microcephaly, periventricular calcification [2], and eye abnormalities such as microphthalmia and optic

nerve atrophy [5]. Of the other infected infants nearly 10% have subclinical congenital infection but will subsequently develop brain disorders including mental retardation, sensorineural hearing loss, visual defects, seizures and epilepsy [6,7]. In adults, infection with human CMV (HCMV) is asymptomatic in immunocompetent hosts, but the virus causes severe or fatal disease in immunocompromised patients [8,9]. CMV has become the most frequent opportunistic cerebral infection in acquired immunodeficiency syndrome (AIDS), in which it results in CMV encephalitis/encephalopathy such as ventriculo-encephalitis [10–12]. The brain is a major target in congenital CMV infection and immunocompromised patients [9].

CMV infection demonstrates a strict host cell type and species specificity [13–15]. As a consequence of the difficulties associated with studies of the pathogenesis of HCMV infection in humans, murine CMV (MCMV) was chosen as a model for HCMV infection. The major reason for using MCMV as a model is the matching biological characteristics of these virus infections in their natural setting. Both MCMV and HCMV cause

\*Corresponding author: Dr Y. Tsutsui, Department of Pathology, Hamamatsu University School of Medicine, 1-20-1 Handayama, Hamamatsu 431-3192, Japan. E-mail: ytsutsui@hama-med.ac.jp

#### Abbreviations used

CMV, cytomegalovirus; CNS, central nervous system; CP, cortical plate;  $\beta$ -gal,  $\beta$ -galactosidase; GFAP, glial fibrillary acidic protein; X-Gal, 5-bromo-3-chloro-indolyl- $\beta$ -galactoside; HCMV, human cytomegalovirus; IE, immediate-early; MCMV, murine cytomegalovirus; NMDA, N-methyl-D-aspartate; NSE, neuron-specific enolase; NSPC, neural stem/progenitor cells; SVZ, subventricular zone; TUNEL, terminal deoxynucleotidyl transferase-mediated dUTP nick end labeling; VZ, ventricular zone.

severe infections in the immunocompromised or immunologically immature host, resulting in similar clinical syndromes [16]. Both viruses have large genomes consisting of about 230 kilobase pairs (kbp) retaining colinear genome organisation: HCMV (AD169) was 229354 bp [17], whereas MCMV (smith strain) was 230278 bp [16]. Both the HCMV and MCMV genomes contain 165–170 predicted open reading frames (ORFs) [16,18]. Despite significant differences in the overall arrangement of the genomes of MCMV and HCMV, the genomes are very similar at the genetic and nucleotide composition level [16].

Model systems have been developed for brain abnormalities induced by infection of mouse embryos with MCMV [19–21]. Based on these models, this review focuses on the effects of MCMV infection on embryogenesis and brain development, and also on neural proliferation and differentiation. These studies may provide basic mechanisms for neuropathogenesis of brain disorders induced by CMV in the human.

#### SUSCEPTIBILITY OF DEVELOPING MOUSE BRAINS TO MCMV

In the early embryonic stage in the mouse, no sign of infection was detected after injection of MCMV into blastocysts and returning them to the uterus [22,23]. Early embryos were also not susceptible to Moloney murine leukemia virus [24] and relatively resistant to West Nile virus (WNV) [25]. It is possible that early embryos may be protected from CMV infection for preservation of the species.

In congenital CMV infection in humans, the brain is the preferential site of infection resulting in sequelae such as microcephaly and microphthalmia as morphological abnormalities, and sequelae such as mental disorder or epilepsy as functional disorders [9,26]. However, little is known about the timing of brain susceptibility to CMV and the susceptible cells in the brain. As an experimental system, the susceptibility of the developing brain to MCMV has been shown in mice by infection of MCMV into embryos through the placenta or by intraperitoneal infection of the virus into the fetus.

The placenta is regarded as a site of congenital CMV infection and infection of the placenta is thought to be a necessary step for transmission of CMV infection into fetuses [27,28]. It has been

reported that transplacental transmission with MCMV does not occur in the mouse [29] presumably because of the three trophoblastic layers of the mouse placenta, which is different from the placentas of human and guinea pigs. In order to simulate transplacental infection to fetuses, mouse placentas at embryonic day 12.5 of gestation (E12.5) were injected directly with MCMV, then the embryos were allowed to develop until E18.5 [21]. The frequency of infection in the brains was prominent in the embryos with placental infection, which was the same as that in the liver and higher than that in the lungs (Figure 1A). In the embryonic brains, the cerebral ventricular zone is the most susceptible site for MCMV infection (Figure 1B). Developmental retardation with microcephaly was sometimes observed in offspring exposed to the placental infection (Figure 1C). Although the ventricular wall has been thought to be a target of congenital CMV infection in humans [2,26] and in animal models [20], direct evidence was provided that fetal brains can be infected by placental infection in mice.

It is known that the susceptibility of mice to MCMV infection *in vivo* diminishes with age [30]. When fetal and neonatal mice were injected intraperitoneally with MCMV during the course of development, fetal and perinatal mice were the most susceptible to MCMV infection [31]. Therefore, the earlier in the developmental stage of the mouse, the more susceptible is the brain to MCMV infection in this experimental system. The brain may acquire some factors for resistance to CMV infection during development, which diminishes susceptibility.

#### NEURAL STEM/PROGENITOR CELLS AS TARGETS FOR SUSCEPTIBILITY

Resistance to susceptibility to CMV has been thought to be due to development of host defense mechanisms such as those mediated by natural killer (NK) cells [32] and macrophages [33] including microglia. It is rather difficult to standardise experimental conditions for *in vivo* analysis of brain susceptibility to virus infection. However, the susceptibility of cells to CMV infection *in vivo* is markedly different from that *in vitro* [8].

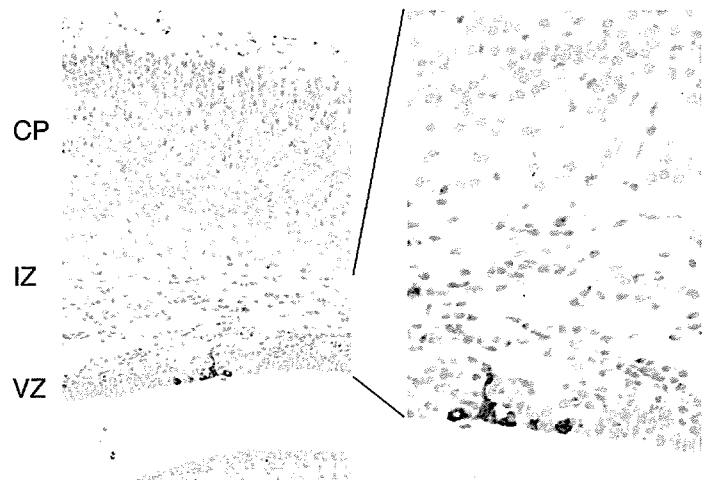
#### Susceptibility in brain slice cultures

Brain slice cultures provide a useful experimental system because they preserve the three-dimensional

### A Placentas and fetus after placental infection with MCMV

	MCMV		MEM	
	PCR (%)	IHC (%)	PCR (%)	IHC (%)
Placenta	22 / 36 (61.1)	16 / 26 (61.5)	1 / 13 (7.7)	0 / 6 (0)
Fetus	13 / 36 (36.1)	8 / 26 (30.8)	0 / 10 (0)	0 / 10 (0)
Brain	10 / 36 (27.8)	7 / 26 (26.9)	0 / 10 (0)	0 / 10 (0)
Lung	7 / 36 (19.4)	4 / 26 (15.4)	0 / 3 (0)	0 / 10 (0)
Liver	10 / 36 (27.8)	7 / 26 (26.9)	0 / 10 (0)	0 / 10 (0)
Survival rate	36 / 62 (58.1)		29 / 48 (60.4)	

### B MCMV-infected cells in fetal brain



### C Postnatal mice and brains

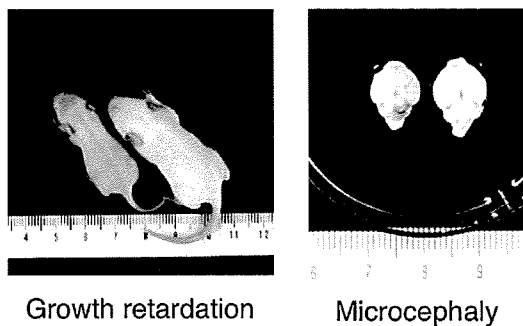


**Figure 1.** Mouse fetuses and brains after placental infection with MCMV. (A) Numbers of infected placentas and fetuses. At day 12.5 of gestation (E12.5), MCMV ( $1 \times 10^3$  PFU) was injected into placentas of the right uterine horn and MEM was injected into placentas of the left horn. The placenta and fetuses were examined at E18.5 by PCR for viral genome and immunohistochemical staining (IHC) for viral antigen. (B) Immunostaining of MCMV-infected cells in the fetal brain at E18.5. CP (cortical plate), IZ (intermediate zone), VZ (ventricular zone). (C) Growth retardation and microcephaly in 7-day-old offspring mice after placental infection with MCMV at E12.2

architecture and the local environment of the brain cells [34], including neurons, glial cells and other immune cells, to a greater extent than dissociated cell cultures. In addition, they permit experimental manipulations and observations to be performed [35]. The effects of MCMV infection on developing mouse brains was investigated in terms of susceptible cells and age-related resistance to MCMV in brain slice cultures [36,37]. Brain slices from BALB/c mice at different developmental stages were infected *in vitro* with recombinant MCMV (RM461) in which the lacZ gene was inserted into a late gene (provided by Dr E.S. Mocarski, Stanford University) [38]. The infected cells can be detected by X-Gal (5-bromo-4-chloro-3-indolyl- $\beta$ -galactoside) and  $\beta$ -gal ( $\beta$ -galactosidase) expression and was visualised as blue spots on brain slices. The subventricular zone (SVZ) and cortical marginal region were the sites most susceptible to MCMV infection, and the susceptibility declined with the develop-

ment of the brain as seen *in vivo* (Figure 2A). It has been reported that resistance to MCMV infection is due to the development of host defense mechanisms such as NK cells [32]. The NK protection against MCMV infection is in part related to a defined resistance gene locus, *Cmv-1*, mapping to chromosome 6 in the NK complex region [39,40]. It was reported that C57BL/6 mice, which have the *Cmv-1* resistant allele, are less susceptible to MCMV infection than BALB/c, which do not have the allele. However, the susceptibility to MCMV infection of brain slice cultures from BALB/c mice was not different from that of slices from C57BL/6 mice [37]. Furthermore, the susceptibility of the developing brains to MCMV in immunocompromised SCID mice was not different from that of BALB/c mice although the mortality rate of SCID mice was substantially greater than BALB/c mice [41]. This Beige-SCID mouse is deficient in both T and B cell functions and has reduced natural killer

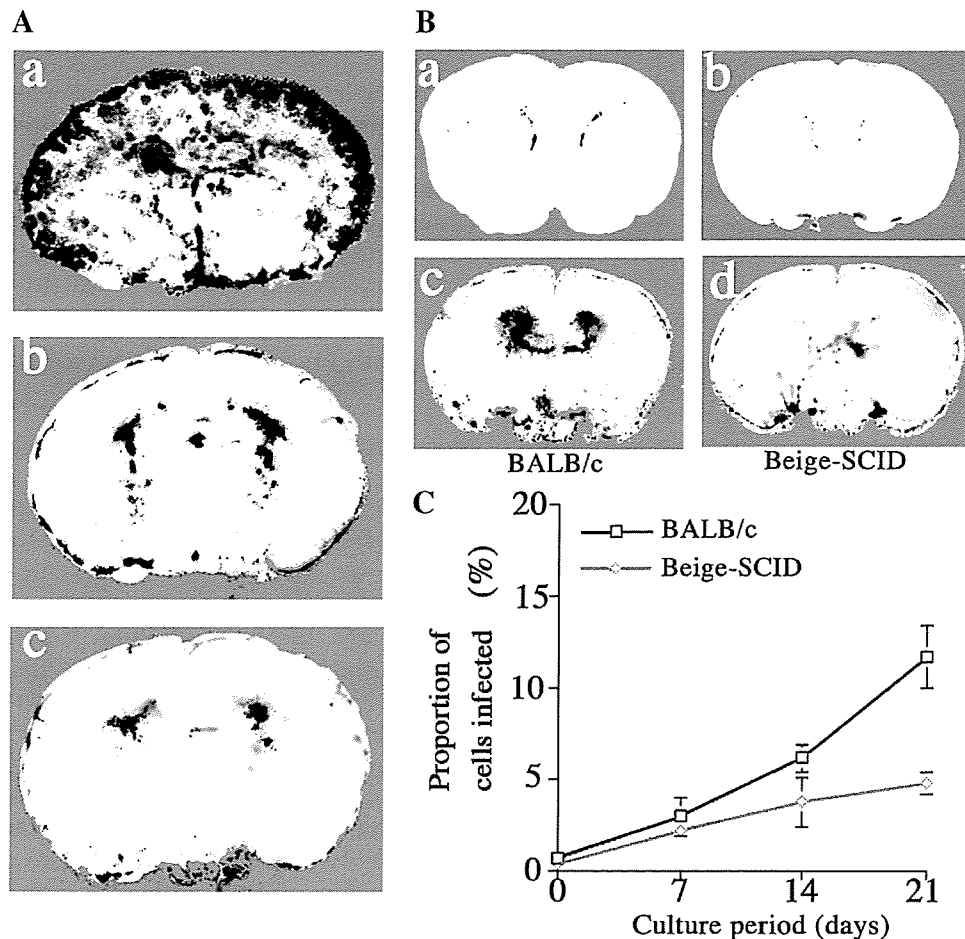


Figure 2. (A) Age-dependent changes of  $\beta$ -Gal expression in the brain slice cultures from mice of different ages after MCMV infection. The brain slice cultures from 7-day-old (a), 14-day-old (b) and 21-day-old (c) BALB/c mice were infected with recombinant MCMV (RM461) ( $5 \times 10^6$  PFU/ml) *in vitro*, and cultured for 5 days, fixed and stained with X-Gal. (B) Increase of infected cells by prolonged culturing prior to MCMV infection. Brain slices from 21-day-old BALB/c mice (a, c) and Beige-SCID mice (b, d) were cultured for 0 day (a, b) and 21 days (c, d) prior to infection with mutant MCMV (RM461). After infection the slices were incubated for 5 days. The number of X-Gal-positive cells increased when the culture period was longer prior to infection. (C) Comparison of the susceptibility of brain slices from BALB/c with that of slices from Beige-SCID mice. Quantitative analysis of proportion of cells infected in brain slices from BALB/c and Beige-SCID mice 5 days after infection by estimating the X-Gal-stained area per whole brain slice area by using Photoshop image software

cell activity [42]. The cells susceptible to MCMV in the ventricular zone proliferated when the brain slices were cultured for a prolonged time. Unexpectedly the amount of proliferation of the susceptible cells was lower in the Beige-SCID mice than in the BALB/c mice [43] (Figure 2B, C). It is possible that immunologic defense mechanisms to MCMV infection work poorly in the developing brain, independent of whole systemic immune system.

Immunostaining showed that virus-susceptible cells in the subventricular zone (SVZ) and cortical marginal regions were positive for nestin, Musashi

and glial fibrillary acidic protein (GFAP), and that most of the infected cells were positive for the proliferating cell nuclear antigen (PCNA) and labeled with bromodeoxyuridine (BrdU) [37]. Thus, the SVZ is the most susceptible site in the brain to MCMV infection and the susceptible cells in the regions are immature neural cells, including neural stem/progenitor cells. Most of the cells in the SVZ consist of undifferentiated neuroepithelial cells, which include neural stem/progenitor cells [44–46]. These cells express neural stem cell markers such as nestin and Musashi [47,48] and also

GFAP [45]. However, these neural stem cell markers were reported to be expressed also in neural progenitor cells and immature glial cells [46]. Therefore, it is possible that cells susceptible to MCMV in the SVZ are immature glial cells and neural progenitor cells, including neural stem cells. It was also reported that in the experiments with rhesus macaques, the spectrum of cortical anomalies and the distribution of infected cells in the fetal brain tissue indicated that immature neuronal cells were preferential targets for rhesus CMV (RhCMV) infection [49]. Furthermore, the targets for human herpesvirus 6 (HHV-6) were reported to be human glial precursor cell culture [50] and targets for coxsackievirus B3 are immature neural cells in the developing brains of BALB/c mice [51].

#### Susceptibility of neurospheres to MCMV

Since immature neural progenitor cells are important factors in the determination of susceptibility of the developing brain to MCMV, the effect of MCMV on the proliferation and differentiation of neural stem cell cultures was analysed according to the method of Reynolds and Weiss [52,53]. In the ventricular zone, multipotential neural stem cells have been identified *in vivo* and *in vitro*, and were shown to be capable of proliferation, self-renewal and to have the potential to differentiate to neuronal or glial precursors [47,54]. The isolated primary brain cells are able to proliferate from single cells to form multipotential spherical cell masses called neurospheres in the presence of epidermal growth factor (EGF). Later neurospheres were proved to be composed of not only neural stem cells but also neural progenitor cells [46,55]; therefore, cells in neurospheres are better named neural stem/progenitor cells (NSPC).

When neural stem/progenitor cells were infected with MCMV as single cells and cultured, the shape of the neurospheres was distorted, viral antigens were expressed in the cells of neurospheres (Figure 3A), and then infectious viruses were released from the neurospheres as detected by plaque assay [56]. It was found that neural stem/progenitor cells are permissive for MCMV infection, although MCMV replication was slower than in mouse embryonic fibroblasts (Figure 3, left upper). MCMV infection inhibited the growth (Figure 3B, right upper) and DNA replication of the neural stem/progenitor cells. A clonogenic

assay revealed that MCMV infection suppressed the generation of colonies from single stem cells (Figure 3, left lower). Because a single cell having the potential to form a neurosphere is thought to be a neural stem cell but not a neural progenitor cell, the results described above may apply only to neural stem cells. It is worth noticing that neural stem cells are susceptible to MCMV infection unlike embryonic stem (ES) cells (in preparation for publication). It has been reported that neural stem cells are different from pluripotent ES cells in terms of genetics and functions [57,58]. These differences between neural stem cells and ES cells remain to be clarified.

In the undifferentiated condition, neurospheres express only nestin but not GFAP and neurofilaments. Neural stem/progenitor cells are induced to differentiate by removing growth factor EGF and adding 2% horse serum, and the differentiated cells are attached on the bottom. Then the expression of nestin is decreased, whereas the expression of neurofilament and GFAP is induced (Figure 3B, right lower). When neural stem/progenitor cells were induced to differentiate after MCMV infection, nestin expression was retained, whereas the expression of neurofilament was more strongly inhibited than that of GFAP in these cells [56]. It is noteworthy that neural stem/progenitor cells tend to retain their undifferentiated condition following MCMV infection. After transplantation into the developing brain, MCMV infection inhibited the migration and neuronal differentiation of the neural stem/progenitor cells [56]. It is possible that CMV infection supports the permissiveness of neural stem cells, inhibits the growth of the neural stem/progenitor cells, and suppresses the neuronal differentiation in addition to disturbing neuronal cell migration. These potential effects may offer an explanation for the developmental disorders of brains associated with congenital CMV infection in humans such as microcephaly.

#### CELL TROPISM OF VIRAL GENE EXPRESSION IN GLIAL AND NEURONAL CELLS

During brain development, neural stem cells commit to induce neural progenitor cells in the ventricular zone (VZ), and migrate to the cortical plate with differentiation to glial or neuronal cells, then forming a cortical layer [59]. It is important to know how CMV infection affects

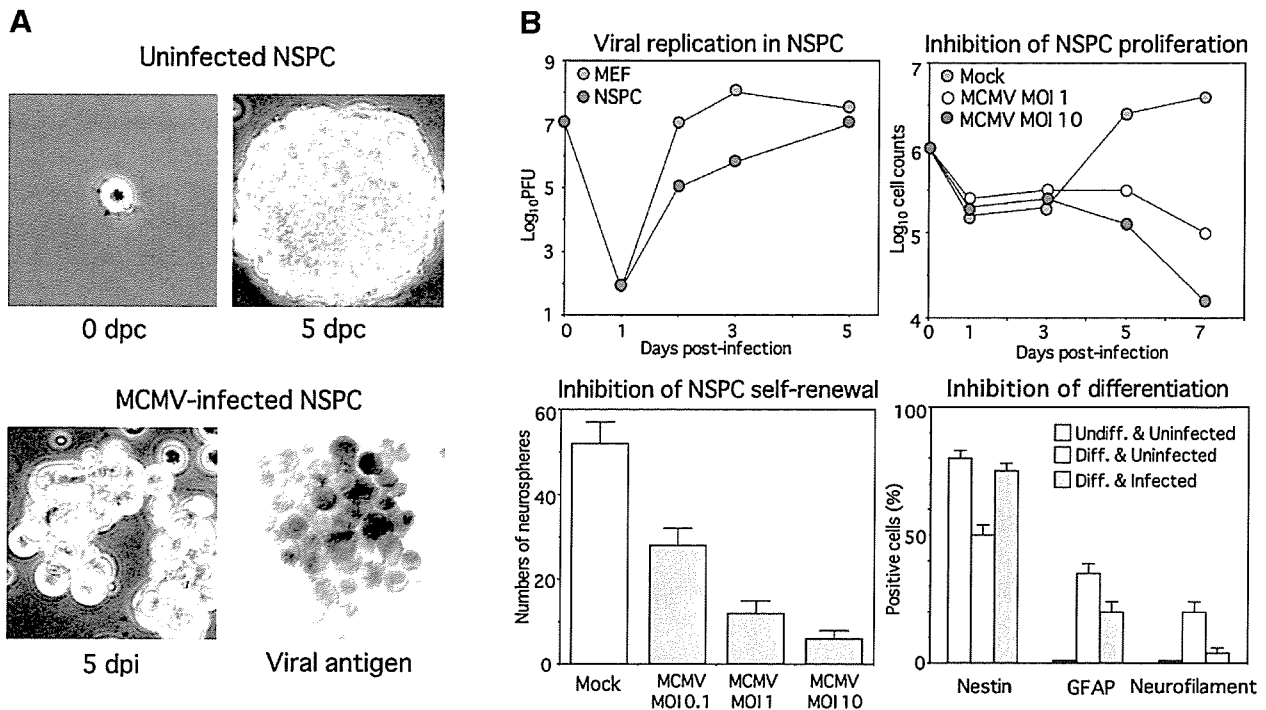


**Figure 3.** Effect of MCMV infection on cultured neural stem/progenitor cells (NSPC) (neurospheres). (A) Effect of MCMV infection on shape and expression of the viral antigen of NSPC. A NSPC from fetal brain (E15.5) formed a neurosphere 5 days after culture (upper). Cells were infected with MCMV as single cells. Shape of neurosphere was disrupted and the viral antigen was expressed 5 days after infection (lower). (B) Comparison of viral titers between NSPC and mouse embryonal fibroblasts (MEF) by plaque assay (upper left). Effect of MCMV infection on growth of NSPC at MOI 1 and 10 (upper right). The clonogenic assay was performed NSPC at different MOIs. The cells were infected when one cell per well in 96-well plates and neurospheres were counted at 7 dpi (lower left). MCMV infection inhibits differentiation of NSPC (right lower). Uninfected and MCMV-infected NSPC were induced to differentiate by removing EGF from the medium but adding 2% horse serum. Undifferentiated (green), differentiated (blue) and MCMV-infected differentiated cells (red) were stained with antibodies specific to nestin, GFAP and neurofilament and the quantity of the antigen-positive cells determined by flow cytometric analysis

the differentiation and migration of neural cells, resulting in brain disorders. For these processes, cell-type specificity of viral infection with different infectious dynamics may be associated with pathogenesis [14,60,61], especially viral gene expression during glial and neuronal differentiation.

The infection dynamics of the neural cells in neonatal mouse brains was analysed in mice infected with MCMV in the late stage of gestation. Specific monoclonal antibodies (mAbs) were made to the MCMV IE1 antigen [62] and to the product of the early gene *e1* (E1) [63]. The cells expressing the IE1 antigen were mostly localised in the VZ, whereas the cells expressing the E1 antigen were diffusely distributed in the cortex and hippocampus (Figure 4A). The IE1-positive cells were preferentially double-stained with anti-GFAP and anti-nestin antibodies: glial immature cells. These cells are thought to be permissive to infection,

because the number of positive cells was similar to that of the viral late gene expressing-cells and viral DNA-positive cells detected by *in situ* DNA-DNA hybridisation. In contrast, the E1-positive cells were double stained with anti-neuron specific enolase (NSE) antibody [62]. This marked contrast in expressing viral antigens in developing brains may depend on differences in the activation of the *ie*-gene promoters between glial cells and neuronal cells. The infected neuronal cells migrated from the ventricular zone (VZ) to the cortical plate (CP) along with brain development (Figure 4B) [64].

#### Immediate-early promoter in transgenic mice

Similar to HCMV and other herpesviruses, CMV genes are expressed in three sequential phases: immediate early (IE), early (E) and late (L) [13,15].

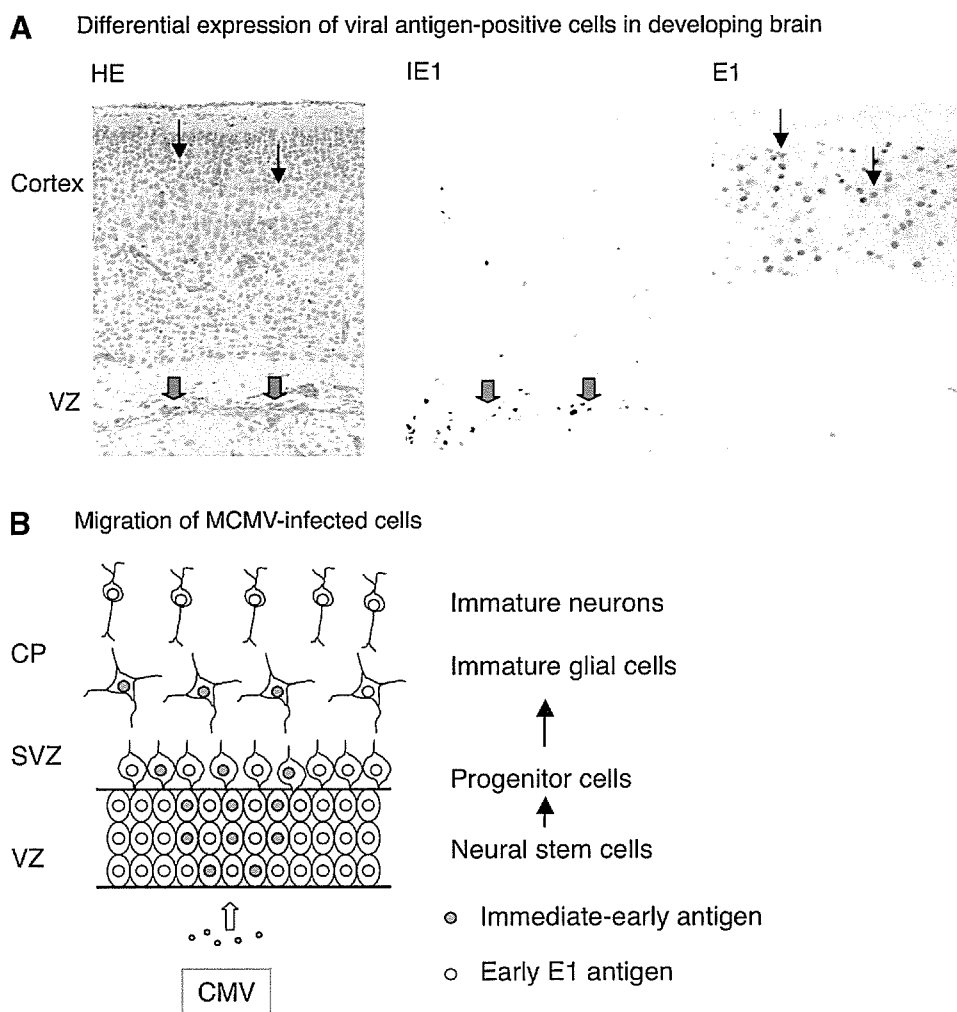
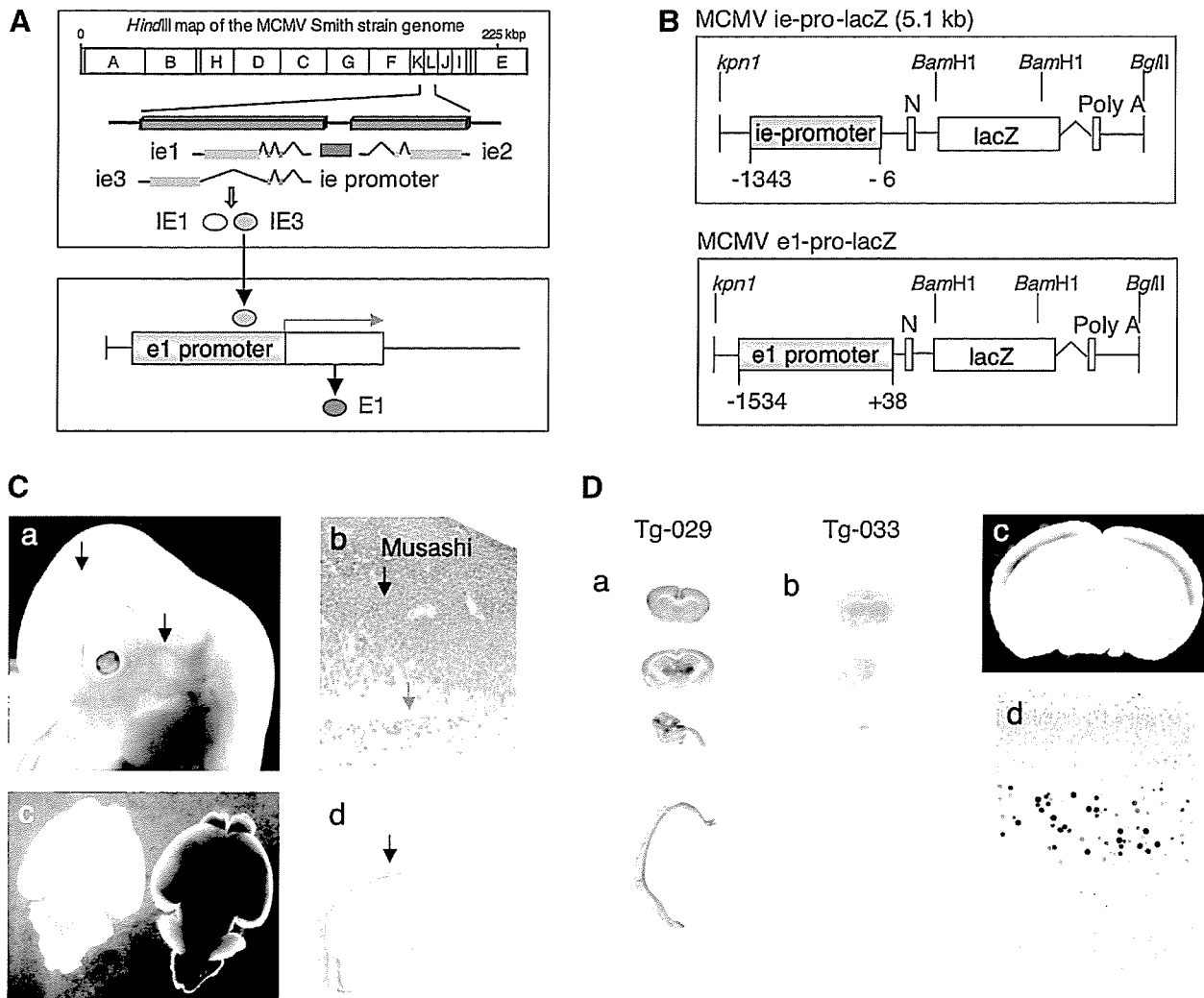


Figure 4. Immunohistochemical comparison between the MCMV IE and E1 antigen-positive cells in developing brains after MCMV infection. (A) The brains were stained with hematoxylin-eosin (HE) (left), with mAbs specific to the IE1 (middle) and E1 antigen (right) in the 7-day-old offspring infected with MCMV on day 15.5 of gestation. (B) Schematic illustration of migration of viral infected-cells from the ventricular zone (VZ) and subventricular zone (SVZ) to cortical plate (CP) during brain development

In HCMV, the most abundantly expressed IE region has at least two immediate-early (ie) genes, called *ie1* (UL123) and *ie2* (UL122), forming a locus that is conserved in other CMVs. MCMV has a predominant IE gene locus that is located in an analogous genomic position to that of HCMV, and is characterised by common structural features (Figure 5A). The two genes that are similar to HCMV *ie1* and *ie2* are referred to as MCMV *ie1* (m123) and *ie3* (M122), respectively [16]. The third gene found in the predominant IE gene, referred to as MCMV *ie2* (M128), is transcribed in the opposite direction from the *ie1* and *ie3* tran-

scripts in this region (Figure 5A) [65]. The MCMV *ie2* gene is not related to a HCMV gene, but it is the positional homologue of HCMV UL 127 gene [66].

Expression of IE genes is highly dependent on appropriate cellular transcription factors that bind to the DNA sequence of the CMV major IE enhancer/promoter [67]. However, by DNA transfection, the major IE (MIE) promoter activates heterogenous genes at high levels in most cultured cell lines [68]. Therefore, the MIE promoter has been used as an expression vector. It has been reported that expression of HCMV MIE



**Figure 5.** Transgenic mice induced with MCMV ie-promoter (Tg ie-pro) and e1-promoter-lacZ (Tg-e1-pro). (A) Schematic illustration of expression of the MCMV ie1 and ie3 by ie-enhancer/promoter (promoter); the product of ie3 gene (IE3) activates e1-promoter to produce the E1 antigen. (B) The constructs of MCMV ie-promoter-lacZ and e1-promoter-lacZ for Tg-ie-pro and Tg-e1-pro, respectively. (C) Activation of  $\beta$ -galactosidase ( $\beta$ -gal) the ie-promoter in vessels (arrows) of the brain of the Tg-ie-pro (E12.5) (a). At this stage, Musashi express in neuroepithelium (black arrow), while the ie-promoter was activated in the endothelium (red arrow) (b). Activation of the ie-promoter was observed in the embryonic brain (E18.5) (c, right), mainly in the ventricular zone (VZ) of lateral ventricle (d, arrow). (D) The transgenic mice with e1-promoter-lacZ (Tg-e1-pro) showed activation of  $\beta$ -gal only in the CNS (Tg-029) (a).  $\beta$ -gal of Tg-033 brain was not activated without MCMV infection (b). Activation of the e1-promoter was observed as layers in cortex (c) and only neuronal cells were stained by immunostaining using anti- $\beta$ -gal antibody (d)

promoter-lacZ genes was cell-type specific in transgenic mice during embryogenesis [69–71]. In adult tissues, transgene was reported to be expressed in neurons, choroid plexus cells and endothelial cells but not in astrocytes unless the cells were stimulated [70].

Transgenic mice were made with the major IE enhancer/promoter involving nucleotides –1343 to –6 (1338 bp) connected to the reporter gene lacZ (MCMV ie pro1-lacZ) (Figure 5B). In adult

mice, transgene expression, as  $\beta$ -galactosidase detected by X-Gal, was detected in the types of cells for which human CMV is tropic such as in distal tubules of the kidney, salivary gland cells, chief cells of the stomach. Interestingly, astrocyte-specific expression of transgene was observed in the brains and in primary glial cultures from the transgenic mice [72]. The spectrum of the expression in organs from MCMV IE promoter was narrow and strictly restricted to particular



cells when compared with that in transgenic mice with the HCMV IE promoter. Host cellular transcription factors may interact with the MCMV IE promoter more naturally in transgenic mice because of the homogeneity of the combination, although transcription factors are evolutionarily well preserved across the species. Alternatively, these observations may have been seen because the MCMV IE promoter region used was 1338 bp in length, far longer than those used for the HCMV IE promoter ( $-524/+13$ ; and  $-67 \pm 54$ ) [69,71]. It has been reported that the HCMV IE promoter may contain a modulator region located between nucleotides  $-750$  and  $-1145$  that negatively regulates the expression of the major IE genes in undifferentiated cells but positively influences the expression in differentiated cells [73,74]. It is possible that the MCMV IE promoter used contained such a region.

Activation of the MCMV IE promoter was analysed in the brain development of the transgenic mice [75]. During the early phase of neurogenesis, the transgene was expressed predominantly in endothelial cells, but not in neuroepithelial cells (Figure 5C, upper). During the later stage of gestation, expression of transgene was largely restricted to the ventricular zone (VZ) (Figure 5C, lower), similar to infected cells *in vivo* [20]. In neural precursor cells induced to differentiate from neurospheres of the transgenic embryo brains, expression of the transgene was detected in glial progenitor cells, expressing GFAP, nestin and Musashi, but not in cells expressing the markers of neuron (MAP2) and oligodendrocyte (myelin-associated glycoprotein: MAG) [75]. In postnatal development, persistent expression was observed in astrocyte-lineage cells. These spatiotemporal changes of MCMV IE promoter activity during brain development correlated with susceptible sites in congenital CMV infection in human [2,26].

#### Early e1 promoter in transgenic mice

In chronic infection of the developing brains in mice, the early nuclear antigen tends to be retained in neurons for a prolonged time after infection using antibody specific to the nuclear antigen (E1) [63]. This nuclear antigen was proved to be the product of MCMV early gene e1 (M112–113) [16] by immunostaining with the transfected cells, corresponding to HCMV early gene (UL112–113) from which nuclear DNA-binding phosphoprotein

is expressed [76]. The products of the MCMV IE genes, especially ie3, were known to activate the early e1-promoter markedly by co-transfection experiments *in vitro* (Figure 5A) [77].

Transgenic mice were generated with an e1 enhancer/promoter region (1572 bp;  $-1534$  to  $+38$ ) connected to lacZ gene (MCMV e1-pro-lacZ) (Figure 6B) [78]. Surprisingly, expression of the transgene was completely restricted to the CNS in all three lines of transgenic mice (Figure 6D). The transgene was expressed in a subpopulation of neurons in the cerebral cortex (Figure 6D, right), hippocampus, diencephalon, brainstem, cerebrum and spinal cord. Non-neuronal cells in the CNS were negative for transgene expression.

It is known that the cascade of expression of the early genes of CMV is induced by the IE gene products together with host cellular factors [15,79]. The results suggest that the MCMV early e1 promoter can be activated in neurons of the CNS by some factors substituting for the IE products. Mocarski *et al.* reported that a deletion mutant of HCMV IE1 replicated under high infective titer conditions [80]. Therefore, it may not be necessary for the viral IE gene to be expressed for activation of the viral early expression in certain situations. Although the brain is the main target in congenital CMV infection and immunocompromised patients, no definite evidence that CMV has a special affinity for the CNS has been reported. The evidence that neuron-specific activation of the MCMV e1 promoter in the transgenic mice may account, at least in part, for the special affinity of CMV for the CNS. It has been reported that neurotropic virus infection in the CNS tends to become persistent in neurons [81]. The CMV IE promoters of both HCMV and MCMV are not well activated in neurons when compared with glial cells [82,83]. Therefore, the acute phase of CMV infection of the brain, in which lytic infection of glial cells is predominant, may convert to the chronic phase of infection in which persistent infection of neurons is predominant. Activation of the E1 gene may be important for transition of neurons to persistent infection.

#### POSSIBILITY OF PERSISTENT INFECTION IN NEURONAL CELLS

It has been reported that CMV causes ventriculo-encephalitis in the developing brain in the acute phase of infection, and that infection then may

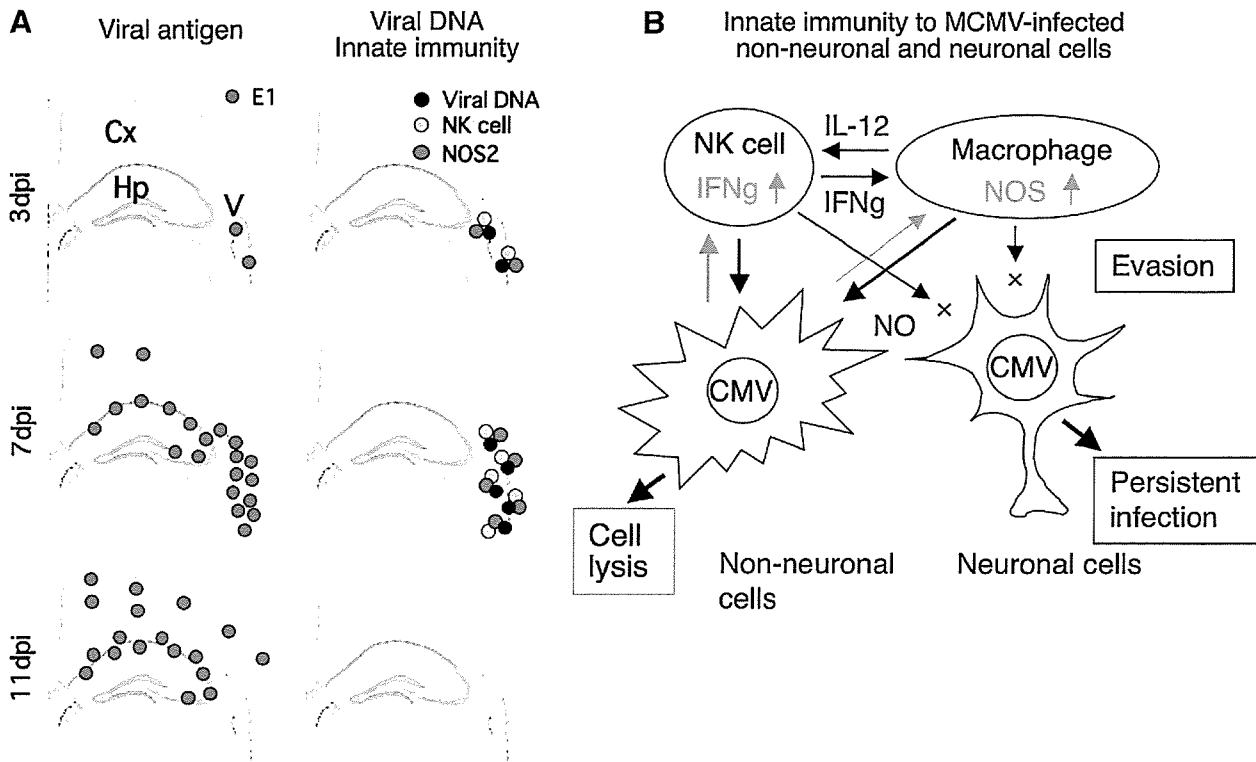


Figure 6. Innate immune responses to MCMV infection in the developing mouse brain and the evasion in the virus-infected neurons. (A) Schematic illustration of expression of the viral antigen. Viral DNA and innate immune reaction in the neonatal brains of newborn mice infected intracerebrally with MCMV. Comparison of cells in the ventricular walls (V) with pyramidal neuron of the hippocampus (Hp) in terms of viral antigen (E1) (blue), viral DNA (black), and NK cells stained with anti-aGM1 antibody (green) and NOS2-positive cells (red) at 3, 7 and 11 dpi. (B) Hypothetical schema concerning the difference in the innate immune response to MCMV-infected cells of non-neuronal cells in the lateral ventricle and MCMV-infected neurons in hippocampus

become chronic or persistent and result in functional neuronal disorders [9,26]. Similarly, MCMV infection in the developing mouse brain begins in the periventricular area and subsequently extends into the cerebral parenchyma and the E1 antigen tends to retain in neurons of the cortex and hippocampus [31,62]. We propose that acute infection in neurons of the developing brain transforms to persistent infection by evasion of innate immunity or anti-apoptotic effect in addition to the neuron-specific activation of the e1-promoter as described below.

#### Evasion of innate immunity

Coexistence of viruses with their hosts imposes an evolutionary pressure on both the virus and the host immune system. The host has developed an immune system able to attack the virus, and viruses have developed evasion mechanisms from this host immune surveillance [84]. Innate

immunity produced by NK cells, macrophages and cytokines acts as a first line of host defense against viral infection. Subsequently, adaptive immunity works to eliminate virus via specific T cells and antibodies [85]. NK cells can secrete interferon (IFN)- $\gamma$ , which not only has direct antiviral activity but can also act by stimulating the expression of nitric oxide synthase type 2 (NO2) in macrophages [86]. NOS2-derived NO appears to be important in the elimination of various viruses including CMV [87,88]. Furthermore, innate immunity seems to be primarily responsible for host defenses against CMV infection, especially during the perinatal period, because of the immaturity of adaptive immunity [89]. There have been several reports concerning the innate immune response during acute CMV infection in liver, spleen, lung, and salivary glands [88]. However, the role of innate immunity to CMV infection of the developing brain remains to be clarified.

From the aspect of defense mechanism, the brain is an immunologically privileged site which is separated from the immune system by the blood–brain barriers [90].

The role of innate immune responses caused by NK cells and NO derived from brain macrophages during MCMV infection in the developing brains of C57BL/6 mice was investigated [91]. The viral titer of the brains of neonatal mice inoculated with MCMV (half of LD<sub>50</sub>) peaked at 7 days post-infection (dpi) then declined. Viral replication in the brain of newborn mice was significantly enhanced by administration of anti-asialo-GM1 antibody, a specific inhibitor of NK cells, or L-N<sup>6</sup>-(1-imminoethyl)-lysine, a specific inhibitor of NO<sub>2</sub>. Thus, NK cells and NO contribute to viral clearance from the brain. At early phases of infection (3 dpi), the MCMV E1 antigen-positive cells and viral DNA were detected in cells of the lateral ventricle (V). At 7 dpi the E1-positive cells were found not only in cells of the lateral ventricle but also in the neurons of the hippocampus (Hp) and cortex (Cx). At a prolonged phase of infection (11 dpi), the E1-positive cells disappeared from the ventricular wall, but persisted in neurons (Figure 6A). At 7 dpi, in the ventricular wall, aGM1 (NK cell marker), NOS (macrophage marker) were expressed markedly, whereas in the hippocampus, although the E1 antigen was expressed in neurons, the markers of NK cells and macrophages were hardly expressed. Viral DNA was also hardly detected in neurons of the hippocampus (Figure 6A, right).

It is hypothesised that some signals from the infected cells in the ventricular walls activate NK cells and macrophages. INF $\gamma$  from NK cells may induce NOS in macrophages, then cytokines such as IL12 from the activated macrophages activate NK cells [86,87], resulting in lysis of the infected cells. In contrast, the prolonged infected neurons in the hippocampus may evade the innate immunity and transfer to persistent infection (Figure 6B). It has been reported that innate immune responses begin with the recognition of MCMV-infected cells by NK cells via the interaction between the Ly49H molecule of NK cells and the m157 protein of MCMV on virus-infected cells [92,93]. It is possible that expression of m157 proteins as ligands for Ly49 receptor of NK cells may be insufficient in MCMV-infected neurons to induce the innate immune response.

Concerning adaptive immunity to virus infected neurons, it was reported that neurons are deficient in major histocompatibility complex (MHC) class I molecules for presentation of viral antigens to specific cytotoxic T lymphocytes and suggested that virus infection would be persistent in these cells [94]. It has been clarified that MCMV encodes a set of genes for prevention or down-modulation of the MHC class I for the viral antigen presentation [95]. Combined with evasion of the innate and adaptive immune responses, virus-infected neurons may tend to become persistently infected cells.

### Anti-apoptotic effect in neuronal cells

Generally, when a virus infects permissive cells, the virus replicates, then infective viruses are released for expansion of infection, while the infected cells are lysed. Virus-infected host cells express apoptotic genes to protect against viral replication and result in apoptosis by themselves. On the other hand, viruses express anti-apoptotic genes to survive, often in the form of persistent infection [96].

It was reported that MCMV infection preferentially persisted in cerebral neurons of the developing mouse brain [31], and that MCMV-infected neurons but not uninfected neurons are resistant to excitotoxic cell death induced by excess glutamate in primary neuronal cultures [97]. Apoptosis was induced in the developing brains by MCMV infection in association with neuronal cell loss. The terminal deoxynucleotidyl transferase-mediated dUTP nick end labeling (TUNEL)-positive cells in the MCMV-infected brains rarely expressed MCMV antigens. In addition, the distribution pattern of the apoptotic cells was different from that of the viral antigen-positive cells and viral DNA-positive cells. These findings suggest that MCMV infection in the developing brains may induce apoptosis predominantly in the non-virus-infected cells. In primary neuronal cultures prepared from embryonic mouse brains, MCMV infection prevented induction of apoptosis by serum deprivation or by glutamate treatment [97]. A similar phenomenon was also reported in a study of a mouse model of CMV retinitis [98]. Many viruses have been reported to evolve mechanisms that block the host apoptotic process, presumably to allow cell survival in stringent conditions for

the virus to grow, resulting in persistent infections [99].

### Possible effect of MCMV infection on neuronal functions

It has been reported that many neurotropic viruses cause persistent neuronal infection without cytopathicity [81,100,101]. Although the exact mechanisms of the viral persistence in neurons are not known, these studies showed that the intracellular milieu of neurons seems to restrict the level of viral gene expression and replication compared with those in non-neuronal cells that are fully permissive for viral replication.

The N-methyl-D-aspartate (NMDA) subtype of glutamate receptors plays an important physiological role in synaptic plasticity and cognitive functions by mediating an influx of  $\text{Ca}^{2+}$  ions through channels gated by these receptors [102,103]. NMDA receptor subunit 1 (NMDA-R1) protein is an essential component of functional NMDA receptors and is widely expressed in the brain [104,105]. It is evident that selective inhibition of the synthesis of NMDA-R1 prevents neuronal cell death induced excitotoxic brain injuries [106]. The amount of NMDA receptors expressed on neurons seems to be an important factor in determining the susceptibility of neurons to excitotoxic cell death.

The effects of MCMV infection on the expression of NMDA receptors was investigated in the hippocampus neurons of neonatal mice and primary neuronal cultures [107]. It was found that MCMV infection inhibits the expression of NMDA-R1 in the hippocampus and primary neuronal culture. The reduction of NMDA receptor expression is likely due to the reduced expression of NMDA receptors in MCMV-infected neurons rather than due to neuronal cell loss, because of scarce presence of TUNEL-positive cells. The reduction of expression of the NMDA-R1 of the CA1 region was more vulnerable to MCMV infection when compared with neurons of the CA3 region [107].

Neuronal excitotoxicity mediated by NMDA receptors has been implicated in the pathogenesis of brain damage induced by lentivirus [108], measles virus [109] and sindbis virus infection [103]. In these studies, it is emphasised that overstimulation of NMDA receptors by excess glutamate or neurotoxins generates apoptotic or necrotic cell death in infected or uninfected neurons. In

our studies, MCMV-infected neurons resist excitotoxic cell death by excess glutamate [107] and inhibition of expression of NMDA receptor, presumably influencing neuronal function, and eventually inducing brain dysfunction.

### LATENCY OF MCMV INFECTION IN BRAIN

A primary CMV infection is followed by a life-long persistence of the virus in a latent state and reactivation may occur later in life. HCMV infection is usually subclinical in immunocompetent individuals, but the virus can cause fatal disease in immunocompromised patients [110]. Latent CMV infection is reported to be in myeloid cells [111], macrophages [112] or lung cells in animal models [113]. Although brain is one of the principal target organs in congenital CMV infection and in immunocompromised patients, little attention has been focused on latent infection and the recurrence of CMV in the brain.

It is hypothesised that the brain disorders occur after recurrent reactivation of the latent infected cells in the brain. In order to test this hypothesis, the reactivation of latent MCMV infection was investigated in mouse brains by transfer to brain slice cultures [114]. It was first shown that latent infection with MCMV occurs in the mouse brain by the procedures. Mutant MCMV (RM461) [38] were infected into perinatal mouse brains and young adult mouse brain of 6-week-old mice and fed for 180 days, enough time for latent infection, then the brains were transferred to brain slice culture, and then cultured up to 4 weeks (Figure 7A). Reactivated cells were detected in the brain slices cultured for 2 to 3 weeks by  $\beta$ -galactosidase ( $\beta$ -gal) staining (Figure 7B). The  $\beta$ -gal-positive cells and infected virus increased during the slice cultures (Figure 7C). Reactivation was observed in about 75% of mice infected during the neonatal period 6 months after infection. Viral replication was also detected by plaque assay. Unexpectedly, reactivation was also observed in 75% of mice infected as young adults, although the numbers of infected cells in the slices was significantly lower than in neonatally infected mice. Interestingly, virus-reactivated cells were observed mainly in immature neural cells in the ventricular walls, expressing markers of the neural stem/progenitor cells such as nestin and Musashi [114].

As reactivation occurred in the brains of mice infected as young adults, it is possible that latent